Carbohydrate Polymers 88 (2012) 734–742

Contents lists available at SciVerse ScienceDirect

Carbohydrate Polymers

journal homepage: www.elsevier.com/locate/carbpol

Microstructure formation of maltodextrin and sugar matrices in freeze-dried systems

Nathdanai Harnkarnsujarit[a,b], Sanguansri Charoenrein[a], Yrjö H. Roos[b,*]

[a] Department of Food Science and Technology, Faculty of Agro-Industry, Kasetsart University, Bangkok, Thailand
[b] School of Food and Nutritional Sciences, University College Cork, Cork, Ireland

ARTICLE INFO

Article history:
Received 3 November 2011
Received in revised form
31 December 2011
Accepted 8 January 2012
Available online 13 January 2012

Keywords:
Collapse
Freeze-drying
Freezing
Maltodextrin
Structure
Sugar

ABSTRACT

Properties of freeze-dried foods are governed by ice formation during freezing. This study investigated the effects of freezing temperature and solids composition on the microstructure and mechanical properties of freeze-dried solids. Maltodextrin and maltodextrin–sugars (glucose, fructose and sucrose) systems were used as solid components. The glass transition and onset temperatures of ice melting for maximally freeze-concentrated systems (T'_g and T'_m) were measured using differential scanning calorimetry. Freezing was carried out at −20, −40 or −80 °C prior to freeze-drying. Microstructural analyses and measurements of mechanical strength in compression were performed using scanning electron microscope and texture analyzer, respectively. The pore size and wall thickness of freeze-dried solids were dependent on the freezing temperature and molecular size of carbohydrates. Sugars depressed the T'_g and T'_m and affected collapse during freeze-drying, but controlled microstructure of non-collapsed solids. The data show differences for freezing processes and compositions that may lead to varying levels of stability of dispersed substances in freeze-dried matrices.

1. Introduction

Microstructure has major roles as the determinant of appearance, functional properties and stability of foods, as emphasized by several authors describing relationships between food properties and structure at macro and molecular levels (Aguilera & Lillford, 2008; Harris & Smith, 2006; Petzold & Aguilera, 2009; Zasypkin, Braudo, & Tolstoguzov, 1997). Structural properties of freeze-dried foods are primarily formed in the prefreezing step and affect, e.g., porosity and strength of solids of freeze-dried foods as well as entrapment of functional food components (Roos, 2010). High porosity gives high rehydration capacity, which is of importance for reconstituted food products. Aguilera and Lillford (2008) pointed out that the size of surface pores also affected the color of freeze-dried coffee.

The sublimation process is strongly affected by pressure, which determines the ice sublimation temperature. The freeze-drying pressure and heat input can be manipulated to obtain an appropriate rate of water removal and a desired porosity and density (Krokida, Karathanos, & Maroulis, 1998; Oikonomopoulou, Krokida, & Karathanos, 2011). Furthermore, various freezing methods have been shown to affect structure formation of freeze-dried polymers differently (Kang, Tabata, & Ikada, 1999; Ma & Zhang, 1999; Madihally & Matthew, 1999; O'Brien, Harley, Yannas, & Gibson, 2005; Shapiro & Cohen, 1997). The smaller pores occupied by ice crystals in rapidly frozen materials give a higher resistance to vapor flow and the freeze-drying may need to be heat transfer controlled, i.e., ice sublimation rate needs to be reduced to avoid internal ice melting and collapse (Pikal, Rambhatla, & Ramot, 2002; Searles, 2010). The possibilities for the manipulation of ice crystal size during freezing are numerous, i.e., the initial ice nucleation conditions can be chosen to control the ice crystal size with subsequent thermal treatment to satisfy ice sublimation requirements during the freeze-drying process. The ice crystal size needs to allow optimum heat and mass transfer properties during dehydration as well as appropriate porosity for product stability and rehydration. During freeze-drying, the ice sublimation temperature needs to be maintained below the collapse temperature, T_c (Bellows & King, 1973; Flink & Karel, 1972), which is known to correlate with the onset temperature of ice melting in maximally freeze-concentrated systems, T'_m (Roos, 1995, 2010). The T'_m values of food components vary substantially and are typically low for sugars, particularly monosaccharides (Roos, 1995, 2010).

The T'_m values of food solids are critical for their successful freeze-drying, as the ice temperature may be controlled by pressure and heat input to maintain a sublimation temperature, $T_s < T'_m$. Collapse in freeze-drying has been shown to be directly related to the decreasing viscosity of amorphous solids as a result of

* Corresponding author. Tel.: +353 21 4902386; fax: +353 21 4276398.
E-mail address: yrjo.roos@ucc.ie (Y.H. Roos).

0144-8617/$ – see front matter © 2012 Elsevier Ltd. All rights reserved.
doi:10.1016/j.carbpol.2012.01.028

plasticization by temperature and unfrozen water above the T'_m (Bellows & King, 1973; Krokida et al., 1998; Levi & Karel, 1995; Tsourouflis, Flink, & Karel, 1976). Collapse occurs as a consequence of exceeding the glass transition temperature (T_g) of the partially freeze-concentrated solids above the T'_m with a rate depending on viscosity of the unfrozen phase and the $T - T_g$ (Bellows & King, 1973; Levi & Karel, 1995; Roos, 1995). Collapse affects significantly the microstructure of freeze-dried foods and may be related to the stability of active components in freeze-dried systems.

The kinetics of bioactive compound degradation and flavor release from dehydrated materials is strongly dependent on dried matrix structure (Desobry, Netto, & Labuza, 1997; Madene, Jacquot, Scher, & Desobry, 2006). The development of functional food ingredients and foods require deep understanding of the critical relationships between food structure, quality, shelf life, delivery characteristics and bioavailability of active components. Freeze-drying is known as the most gentle dehydration method for food and pharmaceutical materials. At favorable freeze-drying conditions, the materials retain their frozen state volume and a highly porous structure results from ice sublimation. Conditions that allow ice melting, however, enhance viscous flow of freeze-concentrated solids and cause structural collapse and loss of porosity (Bellows & King, 1973; Flink & Karel, 1972; Roos, 1995, 2010). Typically a high retention of bioactive substances is achieved in freeze-drying (Desobry et al., 1997; Oungbho & Müller, 1997).

In an earlier study, collapse was found to decrease the rate of β-carotene degradation in freeze-dried mangoes (Harnkarnsujarit & Charoenrein, 2011). The objective of the present study was to investigate the effects of freezing and carbohydrate composition on the structure of freeze-dried solids. The matrices used were maltodextrin and maltodextrin–sugar systems serving as fruit-type food models. Maltodextrin at different dextrose equivalents (DE6, 11 and 25.5) and sugars (glucose, fructose and sucrose) were used. These matrices were frozen using different freezing temperatures and freeze-dried at similar pressure–temperature conditions.

2. Materials and methods

2.1. Maltodextrin and maltodextrin–sugar systems

Agar (microbiology grade, Fluka, Switzerland) was used as a gelling agent to form a semi-solid fruit-like structure containing carbohydrates. Solutions of system components were prepared using maltodextrin (M40, DE6; M100, DE11; M250, DE25.5; Grain Processing Corporation, IA, USA) (18%, w/w), maltodextrin (M100) (9%, w/w) with fructose, glucose, or sucrose (Sigma–Aldrich Co., Germany) (9%, w/w), or sugar mixture (glucose:fructose:sucrose in the ratio of 1:1:4) (9%, w/w) and agar (2%, w/w) in distilled water (80%, w/w). The materials were weighed and dissolved in deionized water (KB Scientific). Solutions with agar were stirred and hydrated using a magnetic stirrer at room temperature (25 °C) for at least 20 min until further heated to 90 °C while stirring and held for 5 min to ensure complete melting of the agar. The gelling solutions were cooled and poured into containers and left for gelation at 25 °C for at least 1 h.

2.2. Freezing and freeze-drying

Samples of all systems were prepared by cutting the gels into cubic (10 mm × 10 mm × 10 mm) samples with a razor blade. The samples were placed on aluminium trays and frozen in still air at −20, −40 or −80 °C for 20 h. All samples subsequently to freeze were tempered at −80 °C for 3 h prior to freeze-drying using a laboratory freeze-dryer (Steris Lyovac GT2, Germany with Leybold Trivac, Germany vacuum pump) for 48 h. This eliminated temperature increases to melt, as the samples were loaded rapidly on freeze-drying shelves operating at room temperature. The chamber pressure was decreased to less than 0.1 mbar corresponding to ice sublimation at $T < -40$ °C. This condition was maintained throughout the freeze-drying to maintain ice temperature below the onset temperatures of ice melting, T'_m, of any of the materials. At the end of freeze-drying, the vacuum was broken using ambient air. The freeze-dried systems were stored in evacuated desiccators containing P_2O_5 for at least 4 days prior to further analysis.

2.3. Freezing profile

A data logger with temperature sensor probes Type T (copper-constantan) (Squirrel SQ800, Grant Instruments Ltd., England) were used to record sample temperatures during freezing. Five ml of the hot agar suspensions were transferred to flat-bottom glass vials (d 4 cm × h 4.5 cm). The vials were sealed with parafilm and left for solidification at room temperature for at least 1 h. The temperature probes were punctured through the parafilm seals and placed in the samples at a height of 0.75 cm from the bottom. The vials were immediately placed on an aluminium tray and frozen at −20, −40 and −80 °C. A temperature probe was also placed on the aluminium tray to record the temperature of the tray during freezing. The freezing temperature data were taken at 10 s intervals at least for 2 h. Triplicate samples were used and the initial cooling rates were read from the initial slopes of the temperature decrease.

2.4. Differential scanning calorimetry

Phase and state transitions of the systems were analyzed with a differential scanning calorimeter (DSC, Mettler Toledo 821e with liquid N_2 cooling). Samples of the freshly prepared hot solutions (25–55 mg) were transferred to preweighed 40 μl DSC aluminium pans (Mettler Toledo, Switzerland) and the pans were hermetically sealed. The DSC was calibrated for temperature and heat flow using n-hexane, mercury, water, gallium and indium, as reported by Haque and Roos (2004). An empty aluminium pan was used as a reference.

Samples in DSC pans were first scanned from 25 to −80 °C (10 °C/min) and held for 2 min, then heated to 25 °C (5 °C/min) to determine the onset temperature of ice melting (T'_m) (Roos & Karel, 1991a). Duplicate samples were then scanned from 25 °C to −100 °C (10 °C/min), held isothermally at −100 °C for 2 min, heated to T'_m −2 °C, held for 15 min, then cooled to −100 °C and held isothermally at −100 °C for 2 min prior to heating to 25 °C at 5 °C/min. The glass transition (T'_g) and onset temperature of ice melting (T'_m) of the maximally freeze-concentrated systems were determined from the final heating scan using STARe Software (Mettler Toledo, Switzerland; version 8.10). The T'_g values were taken from the onset temperatures of the endothermic change in heat flow (heat capacity, C_p) over the glass transition temperature range.

2.5. Scanning electron microscopy

Freeze-dried samples (10 mm × 10 mm × 3 mm thick) were cut with a razor blade and fixed to an aluminium stub using double-sided carbon tape and sputter coated with chromium for 15 min. Samples were examined in a Carl Zeiss Supra 40VP field emission scanning electron microscope (Carl Zeiss AG, Darmstadt, Germany) operating at 10 kV. Digital Images at 8 bit grey level were acquired using the secondary electron detector.

2.6. Texture analysis

The rheological characteristics of the 'anhydrous' freeze-dried systems were obtained using a Texture Analyzer model TA-XT2i

(Texture Technologies, USA). The freeze-dried cubes were removed from the desiccator containing P_2O_5 and immediately compressed with a metal probe (SMS P/50) to a constant deformation (displacement) of 80% (Jaya & Durance, 2009; Nussinovitch, Velez-Silvestre, & Peleg, 1993) at a rate of 0.1 mm s^{-1}. The data were converted to and presented in stress values (kPa) by dividing the compressive force (N) by the sample surface area (0.001 m^2). Peak force and modulus values were calculated using data measured for 5–7 replicate samples.

2.7. Statistical analysis

Compressive force and modulus were subjected to statistical analysis. A one-way analysis of variance (ANOVA) and Duncan's multiple range tests were used to analyze the differences in data at 95% confidence level with SPSS 12.0 Software for Windows.

3. Results and discussion

3.1. Frozen state transitions

The frozen state transitions were dependent on the carbohydrate composition and molecular weight of frozen systems components (Levine & Slade, 1986; Roos, 1995). In the present study, the solutes of the systems were composed of different maltodextrins and maltodextrin–sugar mixtures which showed clear glass transitions of the unfrozen solute phases below the onset temperatures of ice melting at the maximally freeze-concentrated state (Levine & Slade, 1986; Roos & Karel, 1991b). The T'_g and T'_m values are given in Table 1. Annealing at T'_m-2 affected the glass transition by completing ice formation and the T'_g was obtained, but the effect of the isothermal annealing on T'_m was negligible. The glass transition was extremely sensitive to water and the results showed that the annealing effectively increased ice formation (Roos & Karel, 1991b), i.e., increased the T_g to T'_g.

The results showed that the T'_m of the systems were affected by the composition of the solids. Maltodextrins are starch hydrolysis products, which at various DE clearly showed the effect of molecular weight on the T'_m. The higher DE values refer to higher degrees of hydrolysis and higher amounts of smaller molecular weight glucose polymers, including glucose and oligosaccharides. The T'_m decreased with increasing DE and decreasing average molecular weight of the solids. Maltodextrin M40 was of the highest average molecular weight and gave the highest T'_m values, whereas M250 had the lowest average molecular weight and gave the lowest T'_m in accordance with the data of Roos and Karel (1991c). The presence of small molecular weight sugars in a mixture with maltodextrin M100 in a ratio of 1:1 decreased the average molecular weight significantly corresponding to the lower T'_m. Monosaccharides, glucose and fructose, which had the lowest individual T'_m also gave the lowest T'_m for the maltodextrin–sugar mixtures. The results indicated that the lower was the molecular weight of the solids, the lower was the T'_m.

The glass transition of the maximally freeze-concentrated unfrozen solute phase appeared as a small endothermal step below the T'_m. Roos and Karel (1991c) found that the temperature difference between T'_g and T'_m decreased with increasing molecular weight, and the T'_g and T'_m merged for high molecular weight carbohydrate systems. High molecular weight compounds commonly showed a broad glass transition and relatively small change in heat capacity, ΔC_p (Roos & Karel, 1991c). However, the change in heat capacity cannot always be measured for the maximally freeze-concentrated solutes, as the glass transition may overlap with ice melting (Roos, 1993). The glass transitions of sugar systems were more pronounced and could be clearly observed below T'_m. Glucose and fructose had a strong effect on the T'_g of the systems, whereas sucrose had the highest T'_g of the sugar systems. The T'_g of the sugar mixture was closed to sucrose, because of the highest ratio of sucrose (glucose:fructose:sucrose in the ratio of 1:1:4). Sugars effectively depressed the T'_m and T'_g of the maltodextrin–sugar systems. Roos (1993) showed that glucose, fructose and sucrose had T'_m at −46, −46 and −34 °C, and T'_g at −57, −57 and −46 °C, respectively. The T'_m and T'_g values of the sugar systems in the present study agreed with the previous values. However, higher T'_g and T'_m were found when high amounts of maltodextrin (M100) were used with sugars as the system components (Table 1).

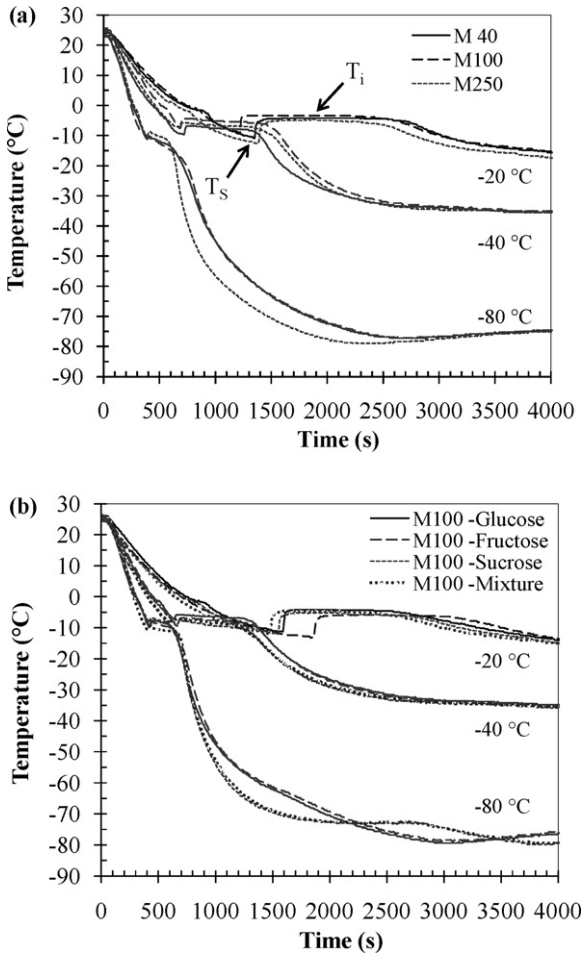

Fig. 1. Freezing profiles of (a) maltodextrin–agar gels and (b) maltodextrin–agar gels with sugars at freezing temperatures of −20, −40 and −80 °C.

Table 1
Glass transition (T'_g) and onset temperature of ice melting (T'_m) of maltodextrin–agar gels with and without sugars, and compression characteristics of freeze-dried solids frozen at −20 °C prior to freeze-drying.

Material	T'_m (°C)	T'_g (°C)	Compression test	
			Peak force (kPa)	Modulus (MPa)
M40 (M_w, 3600)	−13	N/A	65.3 ± 14.6a	9.6 ± 1.4abc
M100 (M_w, 1800)	−16	N/A	57.6 ± 14.2a	7.9 ± 1.2a
M250 (M_w, 720)	−24	N/A	46.0 ± 7.8a	8.6 ± 2.5ab
M100-glucose	−36	−64	159.5 ± 16.4d	11.2 ± 1.7cd
M100-fructose	−37	−64	144.3 ± 19.6d	11.8 ± 1.1d
M100-sucrose	−28	−49	87.6 ± 14.5b	11.9 ± 1.1d
M100-mixture	−31	−55	111.4 ± 19.6c	10.2 ± 1.3bcd

M_w: molecular weight that indicated by the manufacturer.
The values for T'_m and T'_g were ±1 °C.
Different letters show significant differences within the same columns ($p \leq 0.05$).

3.2. Freezing profile and microstructure

The freezing profiles of the maltodextrin systems with and without sugars are shown in Fig. 1a and b. The initial supercooling temperature, T_s, and the freezing temperature at −20, −40 or −80 °C freezing, T_i, as determined from the cooling curves (Fig. 1a and b) are given in Table 2. The T_s and T_i values were insignificantly different for carbohydrates at each freezing temperature. The freezing temperatures of −80 and −20 °C gave similar T_s whereas slightly higher T_s were found at −40 °C. The lower freezing temperature decreased the T_i. These data were used to relate the freezing properties of the systems to their freeze-dried structures. The cooling rates were derived from the initial slopes of the cooling curves to T_s. The system components showed insignificant differences in cooling rates, which were 1.2, 3 and 5.4 °C/min in freezing at −20, −40 and −80 °C, respectively. The cooling rate to T_s was the determinant of the rate of nucleation of water molecules to form ice and showed an increase as the freezing temperature was decreased. The time for the ice crystal growth was temperature-dependent, but almost component independent at all freezing temperatures.

The porous structures of the freeze-dried systems are shown in Fig. 2. The SEM micrographs revealed the interconnected network structure of solids and embedded pores formed by ice crystals during the prefreezing step and vacated as a result of ice sublimation. The direction of pore channels was identical to the formation of dendritic ice crystals (Kang et al., 1999). Heterogeneous pores were found in freeze-dried systems frozen at −20 °C, whereas more homogeneous pores were formed at the freezing temperatures of −40 and −80 °C. The lower freezing temperature and resultant high nucleation rate gave more uniform, smaller and homogeneous pore structures which was in agreement with previous studies (Kang et al., 1999; Ma & Zhang, 1999).

The pore size of freeze-dried systems was reduced as the freezing temperature was decreased to give a higher cooling rate and increased nucleation. Freeze-dried systems frozen at −20 °C had the largest pores and channels as shown in Fig. 2a, d, and g. This higher freezing temperature gave a lower cooling rate, less rapid nucleation and the longest time for ice crystal growth (Fig. 1), and consequently the largest pores left by the ice crystals (Fig. 2). However, the microstructure of the freeze-dried materials was highly dependent on their composition, and the wall membranes represented the unfrozen solute phase formed during prefreezing. The results in Figs. 2 and 3 show that the thickness of the pore membranes decreased as freezing temperature was decreased following the pore size decrease, and corresponding increase in surface area. The inner structure of the freeze-dried systems frozen at −20 °C showed the thickest pore membranes, but also the biggest composition-dependent variations in the number of pores and wall thicknesses (Fig. 3). In contrast, the high cooling rate of freezing at −40 and −80 °C gave thinner wall membranes. The results confirmed that a smaller number of ice nuclei were initially formed at the higher freezing temperature leading to formation of larger ice crystals (Kang et al., 1999). Moreover, Fig. 1 reveals that the time of freezing decreased as the freezing temperature was decreased.

Similar effects of freezing temperature on the pore size of freeze-dried polymers have been reported (Kang et al., 1999; Ma & Zhang, 1999; Madihally & Matthew, 1999; O'Brien et al., 2005; Shapiro & Cohen, 1997). These studies found the decrease in pore size of freeze-dried matrices as freezing temperature was decreased. Van Vlierberghe et al. (2007) demonstrated that at the same final freezing temperature, a decrease of the cooling rate from 0.83 to 0.15 °C/min resulted in a significant increase in the average pore diameter of a freeze-dried gelatin hydrogel. The same study also found that the final freezing temperature between −10 and −30 °C (at the same cooling rate of 0.2 °C/min) did not influence the pore size of the freeze-dried hydrogel (Van Vlierberghe et al., 2007). In the present study, the decreasing pore size of freeze-dried systems, as the freezing temperature was decreased from −20 to −80 °C, was significantly influenced by the increase of cooling rate from 1.2 to 5.4 °C/min. A sufficiently rapid rate of cooling increased the number of nuclei and removed the heat of crystallization, thus preventing the formation of large ice crystals (Kang et al., 1999; Shapiro & Cohen, 1997).

There is still lack of evidence on the effects of composition and freezing properties of solutes (T'_g and T'_m) on the pore size and morphology of freeze-dried solids. The average molecular weight of maltodextrin affected the pore size and wall thickness of freeze-dried solids as well as the presence of various mono- and disaccharides (Fig. 3). An assumption of formation of spherical ice crystals was used to derive the number of ice crystals formed at maximum freeze-concentration of the systems that was maintained throughout freeze-drying. This presumed freezing of water to form an unfrozen phase with 80% solutes and 20% water (Roos & Karel, 1991a; Roos, 1993). Accordingly 75% of the initial weight (volume) was water frozen to ice and 5% of the weight (volume) was unfrozen water. The number of spherical ice crystals that could be formed in each of the 10 mm × 10 mm × 10 mm samples of the 0.75 ml of freezing water is shown in Fig. 3. An expansion of the spheres based on the 0.917 kg/m^3 density of ice could be used to derive the frozen radius of the same number of spheres on which a proportion of the unfrozen fluid (0.25 ml) could form a surface coverage to a final radius with half thickness of the interparticle walls. The wall thicknesses measured for the freeze-dried systems excluding the M40 systems increased linearly with increasing pore diameter, as shown in Fig. 3. It was shown that the wall thickness experimentally and theoretically for spherical pores increased linearly with increasing pore diameter. The linear fit to experimental data showed that 43.5% of the unfrozen fluid was on surfaces and 56.5% was located in interparticle voids. For M40 systems frozen at −80 and −40 °C the unfrozen fluid at particle surfaces increased to 65% but this decreased to 30% when M40 system was frozen at −20 °C locating more unfrozen fluid in the interparticle voids. The results indicated that for maltodextrins a smaller molecular weight gave a smaller pore size and thinner pore membranes at all freezing temperatures. Table 2 showed minor differences in freezing points for maltodextrins, but their molecular size (DE) affected the amount of unfrozen water during freezing at the same temperature and their viscosities could also differ which accounted for the differences in pore sizes. M250 contained a higher amount of small molecular weight solutes retarding ice crystal growth and more unfrozen water during freezing above the T'_m In contrast, M40 had a higher amount of water that formed ice at the same temperature and larger ice crystals were produced during initial freezing.

The pore structures of sugar-containing systems are shown in Fig. 4. Although the cooling rate and freezing temperatures were similar, the results showed that the presence of sugars gave smaller pore sizes to freeze-dried solids (Figs. 2d–4), but followed

Table 2
Freezing properties derived from freezing profiles: supercooling temperature (T_s) and freezing temperature (T_i) of fresh maltodextrin–agar gels with and without sugars frozen at −20, −40 and −80 °C prior to freeze-drying.

Material	−20 °C		−40 °C		−80 °C	
	T_s (°C)	T_i (°C)	T_s (°C)	T_i (°C)	T_s (°C)	T_i (°C)
M40	−11 ± 0	−3 ± 1	−9 ± 1	−6 ± 2	−10 ± 1	−8 ± 3
M100	−10 ± 2	−4 ± 0	−8 ± 2	−8 ± 3	−7 ± 3	−7 ± 2
M250	−12 ± 1	−6 ± 2	−8 ± 2	−10 ± 5	−12 ± 2	−10 ± 3
M100-glucose	−13 ± 1	−6 ± 2	−9 ± 3	−7 ± 2	−9 ± 3	−10 ± 4
M100-fructose	−12 ± 1	−6 ± 1	−9 ± 1	−8 ± 1	−11 ± 2	−12 ± 2
M100-sucrose	−12 ± 0	−5 ± 1	−7 ± 2	−7 ± 2	−8 ± 0	−12 ± 4
M100-mixture	−12 ± 1	−5 ± 1	−9 ± 1	−7 ± 1	−11 ± 1	−11 ± 1

Values shown were mean ± SD of triplicate samples.

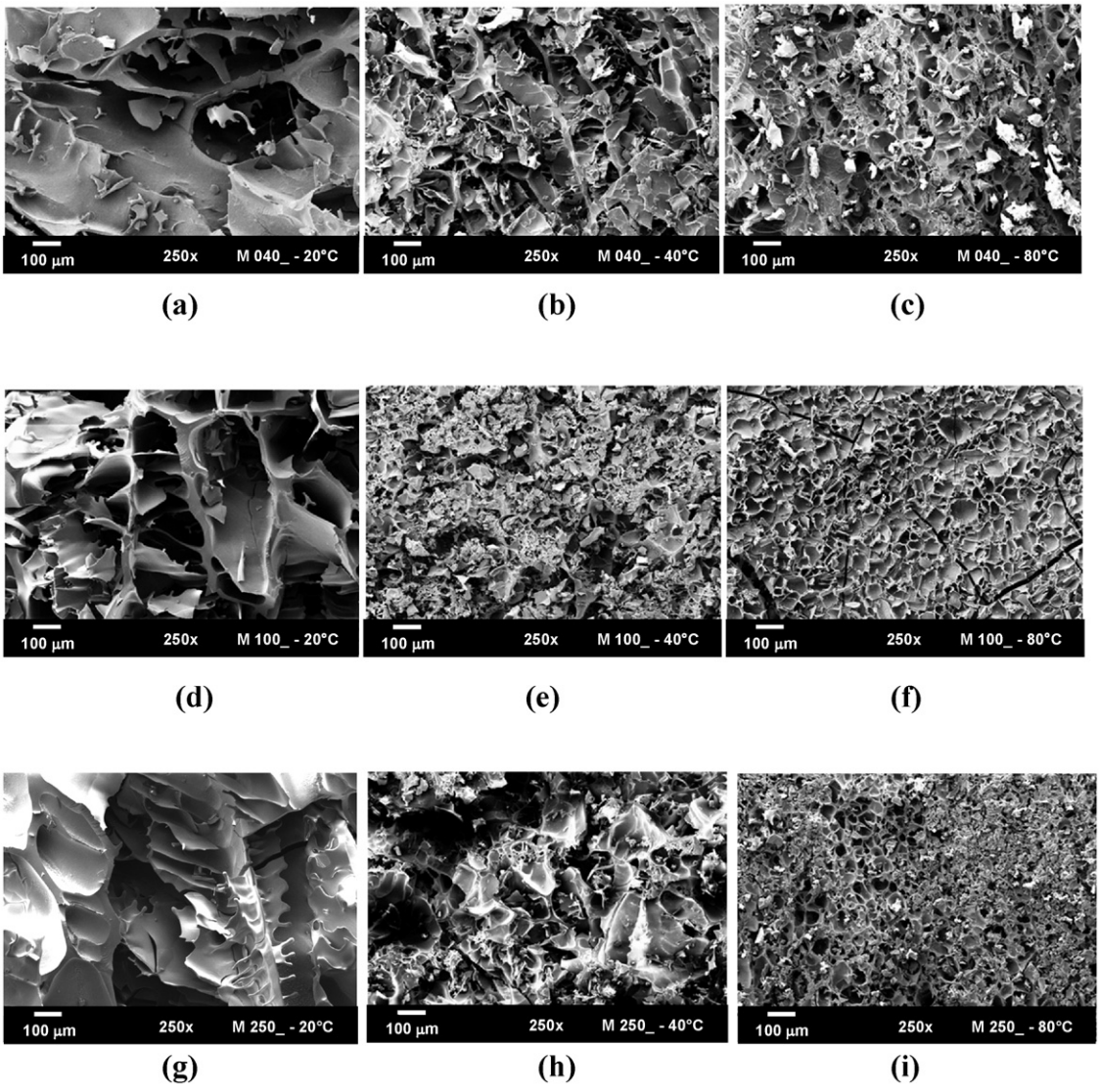

Fig. 2. SEM micrographs of freeze-dried maltodextrin–agar systems: M40 frozen at (a) −20 °C, (b) −40 °C and (c) −80 °C; M100 frozen at (d) −20 °C, (e) −40 °C and (f) −80 °C; and M250 frozen at (g) −20 °C, (h) −40 °C and (i) −80 °C prior to freeze-drying at 250× magnification.

similar surface coverage of the ice crystals by the unfrozen fluid as the M100 and M250 systems. M100-fructose and M100-glucose systems had similar pore structures with heterogeneities (Fig. 4a and b). In contrast, the smaller and more homogeneous pores were observed in M100-sucrose systems (Figs. 3 and 4c). Fig. 3 shows that both the freezing point depression and the glass transition and T'_m properties of the solutes affected ice crystal size and wall thicknesses. Freezing at −20 °C showed crystal growth around equilibrium ice melting temperature (Fig. 1), T'_m, and well above the T'_m of all systems. Upon cooling to −20 °C, higher unfrozen water content remained in systems with the strongest freezing point depression and lowest T'_m. This also affected the temperature difference above the glass transition ($T - T_g$) and viscosity of the unfrozen phase (Roos & Karel, 1991a). As expected, larger pores but thinner walls were obtained for M100-fructose (largest $T - T_g$ at −20 °C) than for M100-glucose. Fructose had a lower T_g and a lower viscosity at the same water content than glucose (Roos, 1993) and formation of larger ice crystals was possible (Fig. 3). However, sucrose had a higher T_g and higher T'_m as well as a smaller freezing temperature depression (higher driving force for nucleation but higher viscosity during crystal growth) which could significantly increase the number of nuclei and reduce crystal size leading to smaller crystals and thinner walls than were formed in M100-fructose and M100-glucose systems. The higher unfrozen water content and lower viscosity of the M100-fructose system allowed formation of larger ice crystals as formation of longer dendrites was possible explaining the smaller wall thickness (Fig. 3). This was also observed for M40 and M100 systems that had a smaller freezing point depression and large pores sizes (enhanced crystal growth) with relatively small wall thickness. The formation of large dendrites in M40 system (Fig. 2a) at the high crystal growth temperature could also increase the heterogeneities of pore walls and concentrate the unfrozen fluid between vertically facing dendrites rather than horizontal walls between dendrites.

Freezing of the maltodextrin systems at −80 and −40 °C showed that a relatively similar freezing point depression, but differences in T'_g and T'_m in freezing at a temperature well below the T'_m affected the rate of nucleation (number and size of pores). M40 systems showed a smaller number and larger pore sizes. It may be expected that nucleation in M40 was retarded in conditions close to maximum freeze-concentration in a shorter time and crystal growth became more rapid, because of a lower DE and higher molecular weight increasing the driving force for the crystal growth after nucleation close to the T'_m conditions. Also a larger quantity of water

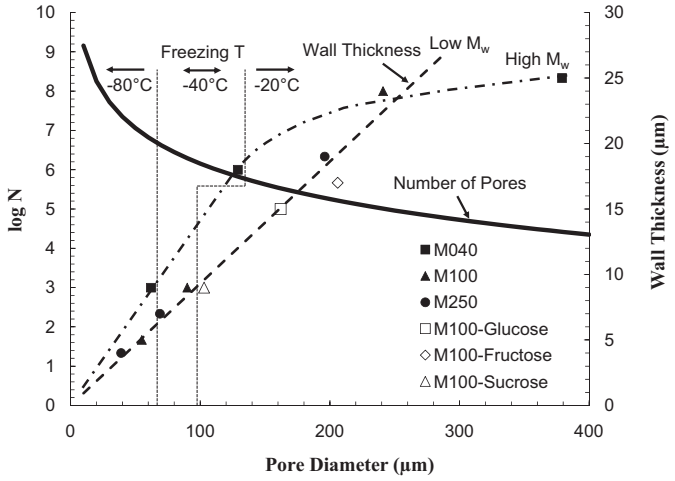

Fig. 3. Number of pores and wall thickness as a function of pore diameter of freeze-dried maltodextrin–agar systems with and without sugars. The number of pores ($\log N$) is given for 10 mm × 10 mm × 10 mm samples. The wall thickness for low molecular weight (M_w) solids correlated with a 43.5% surface coverage of spherical ice crystals by the unfrozen fluid giving the wall thickness shown. A high molecular weight maltodextrin system (M40) had a higher surface coverage of spherical ice crystals at low freezing temperatures.

could crystallize in these systems at the same temperatures than in systems with lower molecular weight further increasing crystal size. This also applied to the differences in the pore sizes and wall thicknesses found for the M100 and M250 systems. It should also be noted that the pore sizes and wall thicknesses in freezing at −40 and −80 °C followed more closely the theoretical values (Fig. 3) confirming that a more rapid nucleation produced smaller, more spherical ice crystals than conditions producing large and more dendrite structured ice crystals.

Interestingly, the DE values of the maltodextrins (molecular size) and the molecular size of the sugars were found to affect the freezing properties and freeze-dried structures of the systems. These materials are commonly used in cryopreservation and as protective matrices in freezing and freeze-drying of pharmaceutical preparations, proteins, bacteria strains and sensitive food components. The results show that the entrapment of dispersed components may become better protected in thicker walls and larger interparticle voids of the high molecular weight carbohydrate systems. These systems are easier to freeze–dry because of the higher T'_m and they are less sensitive to water in the dehydrated state (Roos & Karel, 1991c). However, such high molecular weight components may show less interaction with sensitive components and provide less protection to, for example, native protein structures and cell membranes that may require flexibility during freeze-concentration and freeze-drying.

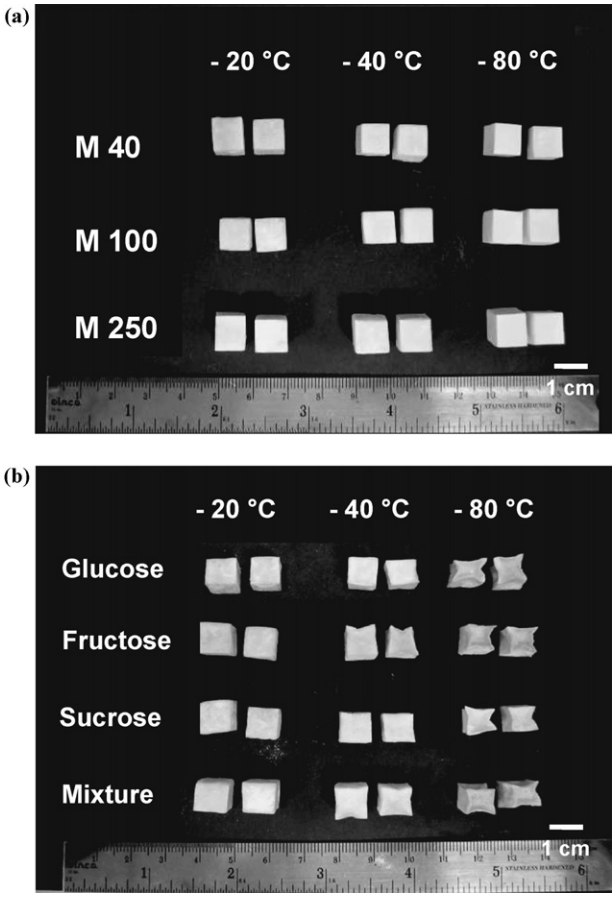

Fig. 5. Appearance of freeze-dried solids: (a) maltodextrin (M40:DE6, M100:DE11 and M250:DE25.5); (b) maltodextrin (M100) with sugar (glucose, fructose, sucrose and mixture) at the ratio of 1:1 frozen at −20, −40 and −80 °C prior to freeze-drying.

3.3. Collapse in freeze-drying

The different freezing temperatures, −20, −40 and −80 °C, showed no significant effects on the macroscopic appearance of the freeze-dried systems (Fig. 5). But some hardening was observed in maltodextrin systems. A similar observation was reported in freeze-dried alginate and agar gels containing starch (Göğüş & Lamb, 1998; Rassis, Saguy, & Nussinovitch, 2002). A rapid cooling of a surface could cause the formation of a crust as water could flow out of the gel and freeze at the surface leaving a shrunken gel (Scherer, 1993). The higher amount of frozen water in M40 system surfaces could lead to a hard crust formation and a high strength to the freeze-dried material. This could also result from

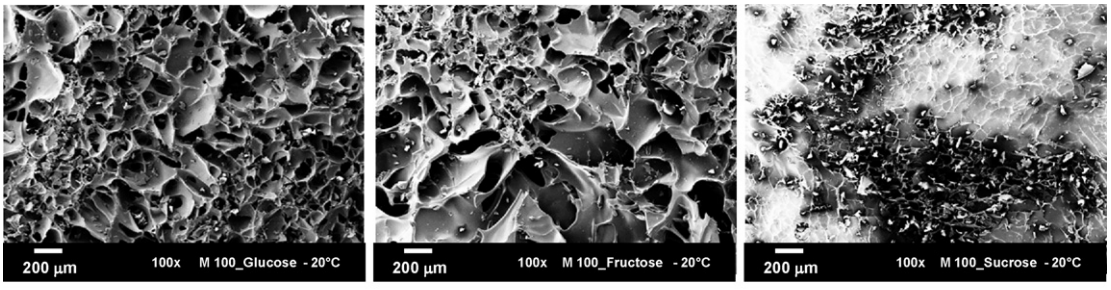

Fig. 4. SEM micrographs of freeze-dried maltodextrin–agar (M100) solids with (a) glucose, (b) fructose, and (c) sucrose frozen at −20 °C prior to freeze-drying at 100× magnification.

smaller pores at the freezing surface of the samples. Sugars gave the structural collapse of freeze-dried solids. Systems frozen at −20 °C had least collapse. As freezing temperature was decreased to −40 °C, structural collapse was clearer but was almost negligible in M100-sucrose systems. The highest degree of collapse resulted from freezing at −80 °C. The degree of collapse was influenced by both freezing temperature and types of sugars, and was particularly the consequence of the pore size effects on mass transfer during freeze-drying.

During freeze-drying, ice supported the frozen structure. Once sublimation removed the ice, the remaining pores did not collapse due to the high viscosity of the concentrated amorphous solution or the unfrozen solutes (Bellows & King, 1972). If the viscosity of the unfrozen solutes decreased to a level that facilitated deformation, the matrix could flow and collapse of the pore could occur (Levi & Karel, 1995). It has been shown that collapse increases above the T_g since the viscosity of the amorphous matrix decreases drastically, as described by the Williams–Landel–Ferry (WLF) relationship (Levi & Karel, 1995; Williams, Landel, & Ferry, 1955). The presence of sugars plasticized the materials and decreased the T'_m and T'_g of the systems. The dried systems, which contained glucose and fructose, had lower glass transition temperatures (T_g) than sucrose (Roos & Karel, 1991c). Therefore, the higher temperature difference between process T and T_g ($T - T_g$) of dried systems containing glucose and fructose also accelerated the structural collapse. The presence of small molecular weight solutes decreased the temperature at which collapse occurred (To & Flink, 1978; Tsourouflis et al., 1976). Rassis et al. (2002) found that there was more total shrinkage of freeze-dried alginate gels, which contained solutes with smaller average molecular size.

As the freeze-dried sugar systems frozen at −40 and −80 °C visually showed structural collapse and loss of porous structure, it was expected that the pores left by small ice crystals gave a high resistance to mass transfer. This could increase ice temperature at the ice interface and result in partial ice melting, which led to plasticization of solids and structural collapse during freeze-drying. The sublimation of small ice crystals resulted in small pores in the dry layer which effectively resisted mass transfer and hence acted as a barrier against sublimation (Pikal et al., 2002). Moreover, the very rapid freezing also caused the crust formation during freezing which produced an additional barrier against vapor flow. As a result, the partial melting of the ice was a major cause for structural collapse during freeze-drying. This led to the high degree of structural collapse during freeze-drying of the systems, which had low T'_m and T'_g and were frozen at low temperature.

The least collapse in sucrose systems, particularly frozen at −40 °C, was caused by the highest T'_m and T'_g of M100-sucrose systems. In contrast, M100 with glucose, fructose and a mixture of sugars showed similar degree of structural collapse at all freezing temperatures because of the similar T'_m and T'_g.

3.4. Texture analysis

Freeze-dried maltodextrin–agar systems frozen at −80, −40 and −20 °C, were analyzed for mechanical strength under compression force using a texture analyzer. The typical compressive stress–strain curves are shown in Fig. 6. When the compressive force was applied, breaking of the brittle pore wall material caused fractures. The freeze-dried systems showed the irregular jagged shape characteristics of a brittle solid foam (Peleg, 1997). These oscillations of stress during compression were denoted as 'jagged' with shape slightly differing among materials due to the wall properties of the pores (Laurindo & Peleg, 2007; Nussinovitch, Corradini, Normand, & Peleg, 2001; Peleg, 1997). Either compressive peak force and/or modulus were found to explain the strength of freeze-dried solids (Hou, Grijpma, & Feijen, 2003; Ma & Choi, 2001; Rassis, Saguy, & Nussinovitch, 1998). The peak in stress–strain curves corresponded to the highest resistance to compression (hardness). Systems frozen at −80 °C were the most resistant to compression followed by those frozen at −40 and −20 °C, respectively (Fig. 7). The higher cooling rate gave higher resistance to compression. This was coincident with the finding of Shapiro and Cohen (1997), who showed that a higher compressive force was needed to deform freeze-dried alginate gels produced by a higher cooling rate using liquid nitrogen freezing. The higher peak forces of systems frozen at low freezing temperature were coincident with the smaller pores and thinner wall membranes. In addition, the very rapid freezing could cause the crust formation and increase the resistance against a compressive force.

Maltodextrin M40 systems had the highest strength at freezing temperatures of −40 and −80 °C. This was caused by the crust formation on the freezing surface during very rapid freezing which

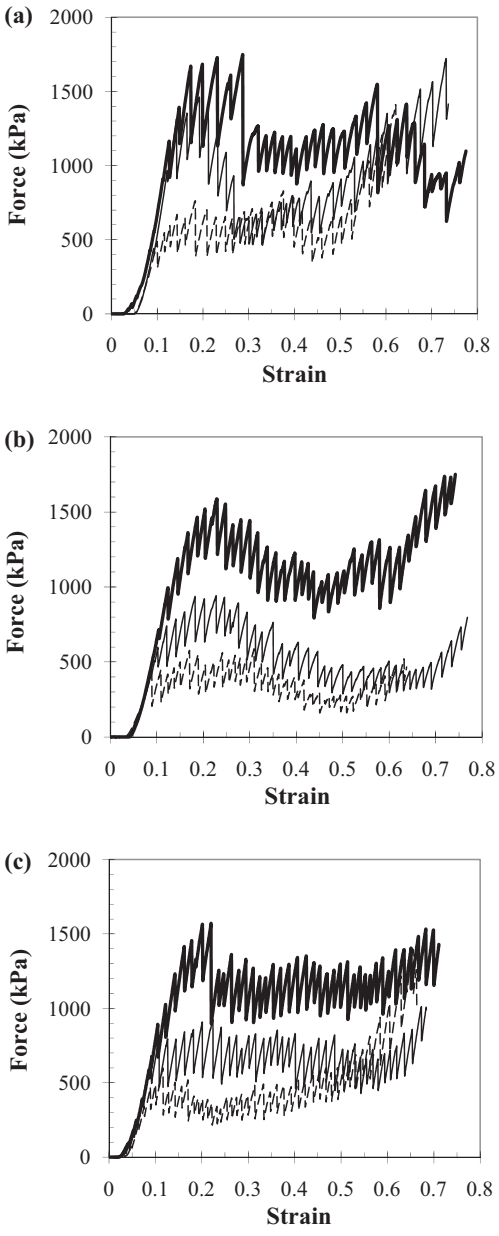

Fig. 6. Compressive force–displacement curves of 'anhydrous' freeze-dried maltodextrin–agar systems: (a) maltodextrin M40:DE6; (b) M100:DE11; (c) M250:DE25.5 frozen at −20 °C (dotted line), −40 °C (normal line) and −80 °C (thick line) prior to freeze-drying.

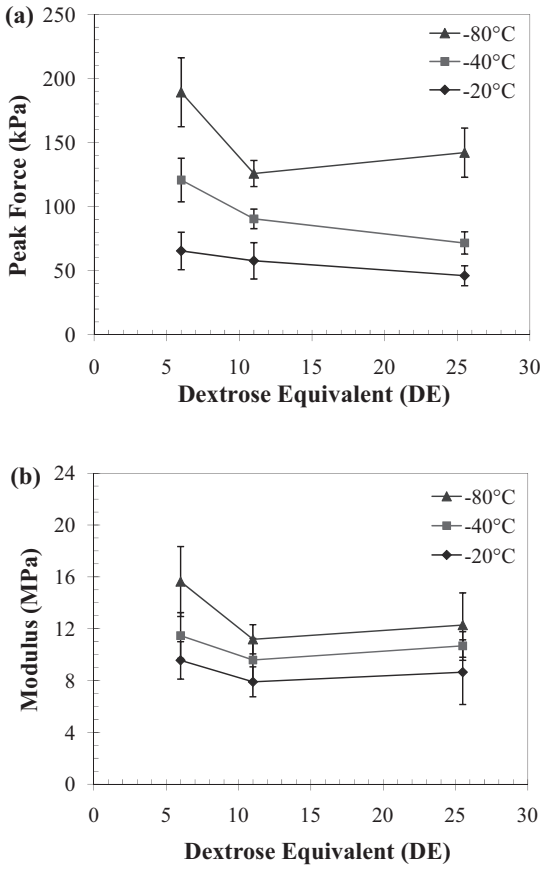

Fig. 7. Compressive (a) peak force and (b) modulus of 'anhydrous' freeze-dried maltodextrin–agar systems (M40, M100 and M250) frozen at −20, −40 and −80 °C prior to freeze-drying as a function of dextrose equivalent (DE).

provided with the strength and enhanced the resistance against compression. The strength of freeze-dried systems composed of M100 and M250 showed only insignificant differences. This was coincident with Corveleyn and Remon (1997) who reported the insignificant differences of maximum penetration force to deform the tablet of xanthan gum, which contained different DE maltodextrins (DE 12, 24 and 38).

The pore size and wall thickness (Fig. 3) affected the strength of the freeze-dried systems. After the maximum peak force plateau, the compressive stress–strain curve showed the typical drop of stress (Fig. 6). The jagged characteristics indicated the strength of pore walls in freeze-dried solids. At above 30% strain, freeze-dried systems frozen at −80 °C clearly revealed the highest force followed by those frozen at −40 and −20 °C, respectively. This reflected the highest strength of pore walls in systems frozen at low temperatures. Although the walls of freeze-dried systems frozen at −80 °C were thinner than at −20 °C, the gap between the walls was smaller owing to the formation of smaller ice crystals. This gave the higher strength to freeze-dried solids. Moreover, the smaller pore size distributed stresses in the system more evenly allowing it to resist the compressive force leading to bigger amplitude of each jagged peak. Therefore, the smaller pore size and increase in the number of pores provided strength against compressive crack propagation under applied compressive force (Kim et al., 2004). Freeze-dried systems frozen at −80 °C revealed the highest strength of the pore walls.

In this study, the amount and concentration of solids were the same. However, systems frozen at −80 °C gave higher compressive modulus than all maltodextrin systems frozen at −20 °C (Fig. 7b), whereas, the systems frozen at −40 °C showed insignificant differences to −20 and −80 °C. The lowest modulus indicated the highest deformation rate, which referred to high brittleness and lower strength of solids. The DE of maltodextrins showed no effect on modulus values.

The compressive peak force and modulus of freeze-dried maltodextrin systems with sugars frozen at −20 °C are shown in Table 1. Sugars increased solid strength as reflected by higher peak force and modulus values than were measured for the M100 system. It is possible that the sugar-containing glass potentially enhanced the strength of freeze-dried solids. Moreover, the small molecular weight sugars interacted compatibly with maltodextrins and/or agar which enhanced the strength of solids. Sucrose-containing dry solids revealed the lowest peak force. Glucose and fructose as components showed no differences in peak forces, whereas mixtures of sugars gave values in between these sugars and sucrose. This was possibly due to the smallest pore size of sucrose-based systems.

4. Conclusion

The results indicated the relationship between process-induced structure formation in freeze-dried carbohydrate solids. The structures of freeze-dried solids were influenced by both freezing temperature and solid properties (freezing point depression, T_g, T'_g and T'_m). The lower freezing temperature increased the nucleation rate of the systems. High cooling rate as well as the higher $T - T'_g$ generated a large number of small ice crystals which led to a smaller pore size and thinner pore walls. Sugars (glucose, fructose and sucrose) depressed the T'_g and T'_m of the systems and caused the structural collapse during freeze-drying of systems frozen at −40 and −80 °C. A higher degree of structural collapse was visually observed in freeze-dried systems frozen at a lower temperature and had a low T'_m. The small ice crystals formed during freezing at low temperatures effectively led to the resistance of vapor flow during sublimation and hence enhanced structural collapse. The freezing temperatures of −40 and −80 °C gave a large number of small pores and affected crust formation in freeze-dried solids which enhanced the mechanical strength against compression. The compressive stress–strain curves revealed a good relationship between mechanical strength and pore size. This study showed that the freezing process as affected by freezing parameters and matrix formulation can be of high significance in the use of different carbohydrates as protective components and structure forming materials in numerous food and pharmaceutical delivery systems.

Acknowledgements

This work was financially supported by the Thailand Research Fund through the Royal Golden Jubilee Ph.D. program (Grant no. PHD/0224/2549) as well as the Food Institutional Research Measure (FIRM) project number 08-RDC-695 funded by the Department of Agriculture, Fisheries and Food, Ireland. The authors thank Dr. Mark Auty for providing facilities and assistance enabling SEM imaging of the freeze-dried materials as well as Mr. Eddie Beatty and Ms. Theresa Dennehy for technical support.

References

Aguilera, J. M., & Lillford, P. J. (2008). Structure-property relationships in foods. In J. M. Aguilera, & P. J. Lillford (Eds.), *Food material science: Principle and practice*. NY, USA: Springer Science & Business Media.

Bellows, R. J., & King, C. J. (1972). Freeze-drying of aqueous solutions: Maximum allowable operating temperature. *Cryobiology*, *9*, 559–561.

Bellows, R. J., & King, C. J. (1973). Products collapse during freeze drying of liquid foods. *AIChE Symposium Series*, *69*, 33–41.

Corveleyn, S., & Remon, J. P. (1997). Formulation and production of rapidly disintegrating tablets by lyophilisation using hydrochlorothiazide as a model drug. *International Journal of Pharmaceutics*, *152*, 215–225.

Desobry, S. A., Netto, F. M., & Labuza, T. P. (1997). Comparison of spray-drying, drum-drying and freeze-drying for β-carotene encapsulation and preservation. *Journal of Food Science*, *62*, 1158–1162.
Flink, J. M, & Karel, M. (1972). Mechanisms of retention of organic volatiles in freeze-dried systems. *Journal of Food Technology*, *7*, 199–211.
Göğüş, F., & Lamb, J. (1998). Choice of model gel systems for the food dehydration studies. *Drying Technology*, *16*, 297–309.
Haque, Md. K., & Roos, Y. H. (2004). Water plasticization and crystallization of lactose in spray-dried lactose/protein mixtures. *Journal of Food Science*, *69*, 23–29.
Harnkarnsujarit, N., & Charoenrein, S. (2011). Influence of collapsed structure on stability of β-carotene in freeze-dried mangoes. *Food Research International*, *44*, 3188–3194.
Harris, P. J., & Smith, B. G. (2006). Plant cell walls and cell-wall polysaccharides: Structures, properties and uses in food products. *International Journal of Food Science and Technology*, *41*, 129–143.
Hou, Q., Grijpma, D. W., & Feijen, J. (2003). Porous polymeric structures for tissue engineering prepared by a coagulation, compression moulding and salt leaching technique. *Biomaterials*, *24*, 1937–1947.
Jaya, S., & Durance, T. D. (2009). Compressive characteristics of cellular solids produced using vacuum-microwave, freeze, vacuum and hot air dehydration methods. *Journal of Porous Materials*, *16*, 47–58.
Kang, H. W, Tabata, Y., & Ikada, Y. (1999). Fabrication of porous gelatin scaffolds for tissue engineering. *Biomaterials*, *20*, 1339–1344.
Kim, U. J., Park, J., Li, C., Jin, H. J., Valluzzi, R., & Kaplan, D. L. (2004). Structure and properties of silk hydrogels. *Biomacromolecules*, *5*, 786–792.
Krokida, M. K., Karathanos, V. T., & Maroulis, Z. B. (1998). Effect of freeze-drying conditions on shrinkage and porosity of dehydrated agricultural products. *Journal of Food Engineering*, *35*, 369–380.
Laurindo, J. B., & Peleg, M. (2007). Mechanical measurements in puffed rice cakes. *Journal of Texture Studies*, *38*, 619–634.
Levi, G., & Karel, M. (1995). Volumetric shrinkage (collapse) in freeze-dried carbohydrates above their glass transition temperature. *Food Research International*, *28*, 145–151.
Levine, H., & Slade, L. (1986). A polymer phisico-chemical approach to the study of commercial starch hydrolysis products (SHPs). *Carbohydrate Polymers*, *6*, 213–244.
Ma, P. X., & Choi, J. W. (2001). Biodegradable polymer scaffolds with well-defined interconnected spherical pore network. *Tissue Engineering*, *7*, 23–33.
Ma, P. X., & Zhang, R. (1999). Synthetic nano-scale fibrous extracellular matrix. *Journal of Biomedical Materials Research*, *46*, 60–72.
Madene, A., Jacquot, M., Scher, J., & Desobry, S. (2006). Flavour encapsulation and controlled release—A review. *International Journal of Food Science and Technology*, *41*, 1–21.
Madihally, S. V., & Matthew, H. W. T. (1999). Porous chitosan scaffolds for tissue engineering. *Biomaterials*, *20*, 1133–1142.
Nussinovitch, A., Velez-Silvestre, R., & Peleg, M. (1993). Compressive characteristics of freeze-dried agar and alginate gel sponges. *Biotechnology Progress*, *9*, 101–104.
Nussinovitch, A., Corradini, M. G., Normand, M. D., & Peleg, M. (2001). Effect of starch, sucrose and their combinations on the mechanical and acoustic properties of freeze-dried alginate gels. *Food Research International*, *34*, 871–878.
O'Brien, F. J., Harley, B. A., Yannas, I. V., & Gibson, L. (2005). The effect of pore size on cell adhesion in collagen-GAG-scaffolds. *Biomaterials*, *26*, 433–441.
Oikonomopoulou, V. P., Krokida, M. K., & Karathanos, V. T. (2011). Structural properties of freeze-dried rice. *Journal of Food Engineering*, *107*, 326–333.
Oungbho, K., & Müller, B. W. (1997). Chitosan sponges as sustained release drug carriers. *International Journal of Pharmaceutics*, *156*, 229–237.
Peleg, M. (1997). Review: Mechanical properties of dry cellular solid foods. *Food Science International*, *3*, 227–240.
Petzold, G., & Aguilera, J. M. (2009). Ice morphology: Fundamentals and technological applications in foods. *Food Biophysics*, *4*, 378–396.
Pikal, M. J., Rambhatla, S., & Ramot, R. (2002). The impact of freezing stage in lyophilization: Effect of the ice nucleation temperature on process design and product quality. *American Pharmaceutical Review*, *5*, 48–53.
Rassis, D. K., Saguy, I. S., & Nussinovitch, A. (1998). Physical properties of alginate-starch cellular sponges. *Journal of Agricultural and Food Chemistry*, *46*, 2981–2987.
Rassis, D. K., Saguy, I. S., & Nussinovitch, A. (2002). Collapse, shrinkage and structural changes in dried alginate gels containing fillers. *Food Hydrocolloids*, *16*, 139–151.
Roos, Y. (1993). Melting and glass transitions of low molecular weight carbohydrates. *Carbohydrate Research*, *238*, 39–48.
Roos, Y. (1995). *Phase transitions in foods*. San Diego, USA: Academic Press.
Roos, Y. (2010). Crystallization, collapse and glass transition in low-water food systems. In D. S. Reid, T. Sajjaanantakul, P. J. Lillford, & S. Charoenrein (Eds.), *Water properties in food, health, pharmaceutical and biological systems: ISOPOW 10*. Oxford, UK: Wiley-Blackwell.
Roos, Y., & Karel, M. (1991a). Amorphous state and delayed ice formation in sucrose solutions. *International Journal of Food Science and Technology*, *26*, 553–566.
Roos, Y., & Karel, M. (1991b). Nonequilibrium ice formation in carbohydrate solutions. *Cryo-Letters*, *12*, 367–376.
Roos, Y., & Karel, M. (1991c). Water and molecular weight effects on glass transitions in amorphous carbohydrates and carbohydrate solutions. *Journal of Food Science*, *56*, 1676–1681.
Scherer, G. W. (1993). Freezing gels. *Journal of Non-Crystalline Solids*, *155*, 1–25.
Searles, J. A. (2010). Freezing and annealing phenomena in lyophilization. In J. C. May, & L. Rey (Eds.), *Freeze-drying/lyophilization of pharmaceutical and biological products*. NY, USA: Informa Healthcare.
Shapiro, L., & Cohen, S. (1997). Novel alginate sponges for cell culture and transplantation. *Biomaterials*, *18*, 583–590.
To, E. C., & Flink, J. M. (1978). 'Collapse', a structural transition in freeze-dried carbohydrates: II. Effect of solute composition. *Journal of Food Technology*, *13*, 567–581.
Tsourouflis, S., Flink, J. M., & Karel, M. (1976). Loss of structure in freeze-dried carbohydrates solutions: Effect of temperature, moisture content and composition. *Journal of the Science of Food and Agriculture*, *27*, 509–519.
Van Vlierberghe, S., Cnudde, V., Dubruel, P., Masschaele, B., Cosijns, A., De Paepe, I., et al. (2007). Porous gelatin hydrogels: 1. Cryogenic formation and structure analysis. *Biomacromolecules*, *8*, 331–337.
Williams, M. L., Landel, R. F., & Ferry, J. D. (1955). The temperature dependence of relaxation mechanisms in amorphous polymers and other glass-forming liquids. *Journal of the American Chemical Society*, *77*, 3701–3707.
Zasypkin, D. V., Braudo, E. E., & Tolstoguzov, V. B. (1997). Multicomponent biopolymer gels. *Food Hydrocolloids*, *11*, 159–170.